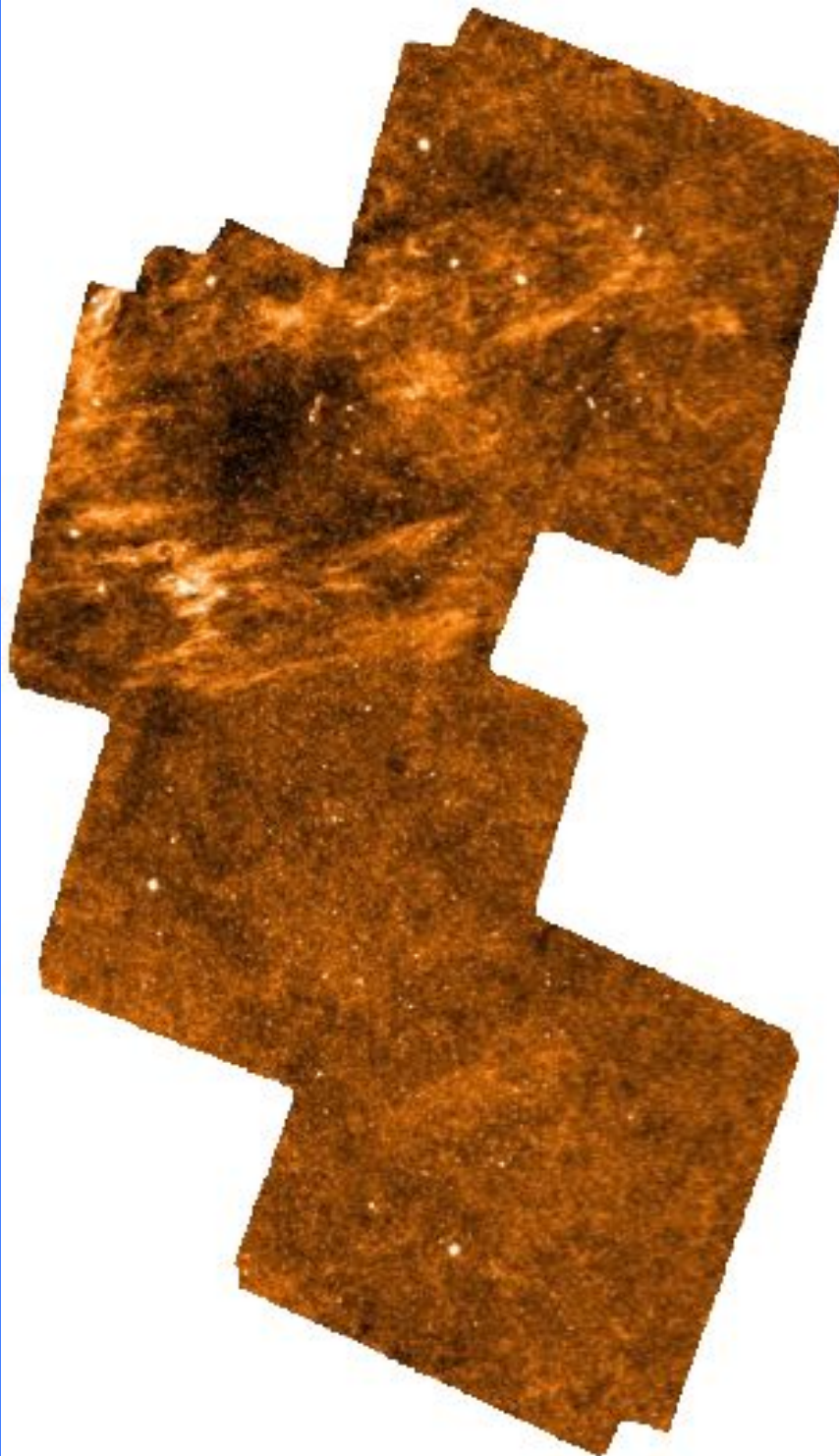


*Herschel
Virgo Cluster
Survey
(HeViCS)*

Jonathan Davies
for the HeViCS consortium

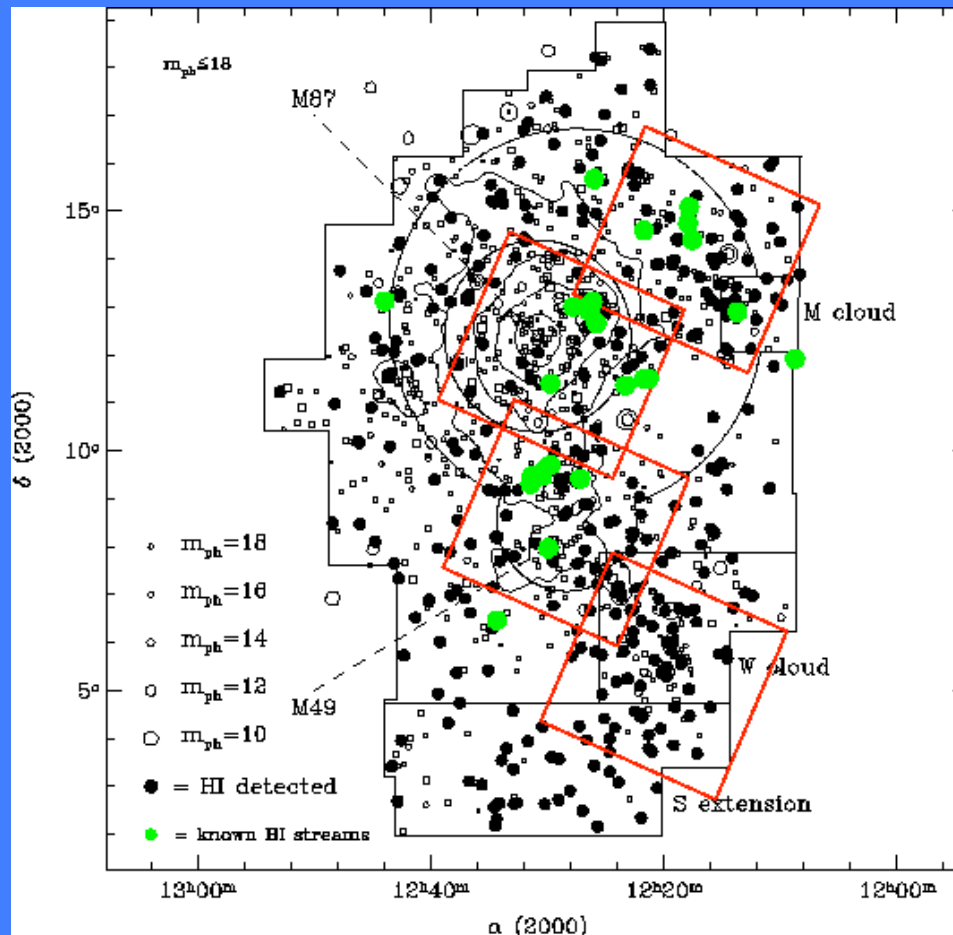


HeViCS

Consortium Members

[Davies, J. I.](#); [Baes, M.](#); [Bendo, G. J.](#); [Bianchi, S.](#); [Bomans, D. J.](#); [Boselli, A.](#);
[Clemens, M.](#); [Corbelli, E.](#); [Cortese, L.](#); [Dariush, A.](#); [de Looze, I.](#); [di Serego Alighieri, S.](#);
[Fadda, D.](#); [Fritz, J.](#); [Garcia-Appadoo, D. A.](#); [Gavazzi, G.](#); [Giovanardi, C.](#); [Grossi, M.](#);
[Hughes, T. M.](#); [Hunt, L. K.](#); [Jones, A. P.](#); [Madden, S.](#); [Pierini, D.](#); [Pohlen, M.](#); [Sabatini, S.](#);
[Smith, M. W. L.](#); [Verstappen, J.](#); [Vlahakis, C.](#); [Xilouris, E. M.](#); [Zibetti, S.](#)





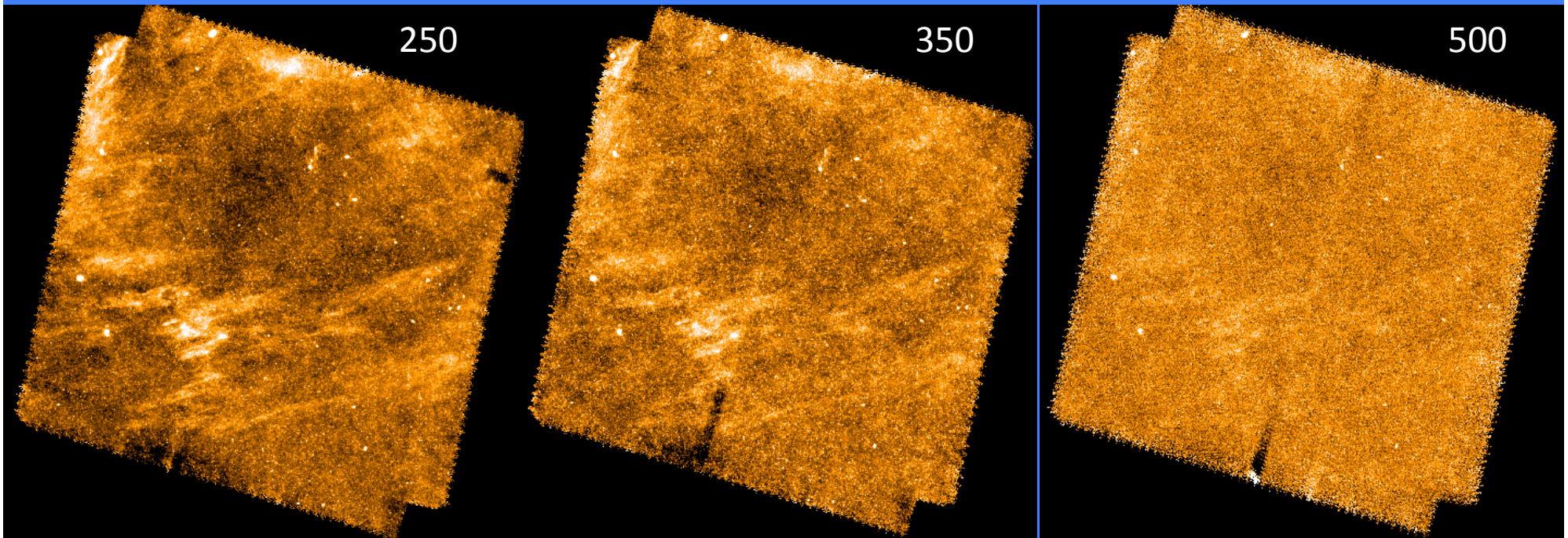
The Proposal

286 hours of SPIRE
 and PACS parallel
 mode to scan 64 sq deg (8 scans)
 of the nearby Virgo cluster
 providing data from PACS at 100 and 160 μ
 and SPIRE at 250, 350 and 500 μ
 Resolution 7-35 arc sec

 SD data is 2 scans of the central
 cluster field
 Noise 3-12 mJ/beam
 Calibration error approx 20% PACS 15% SPIRE

Science Topics

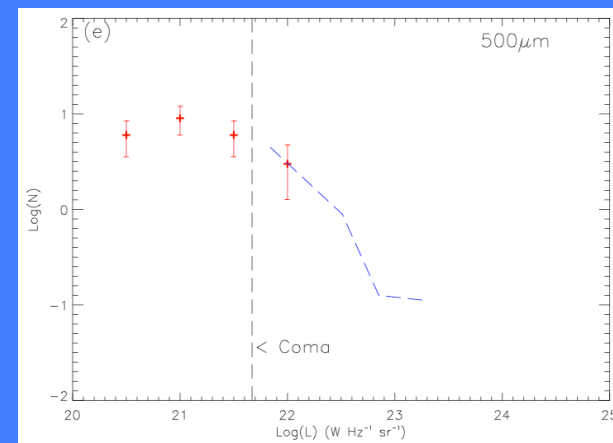
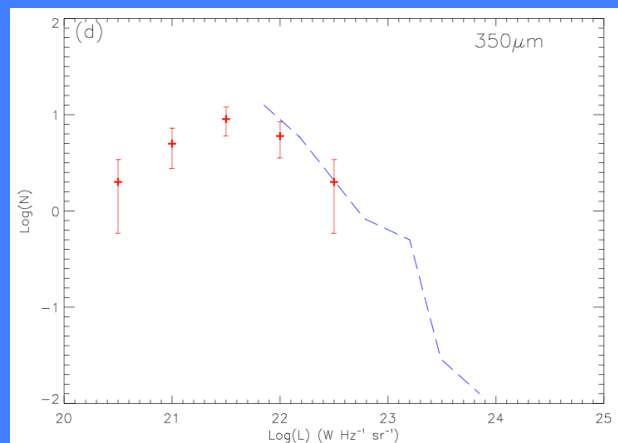
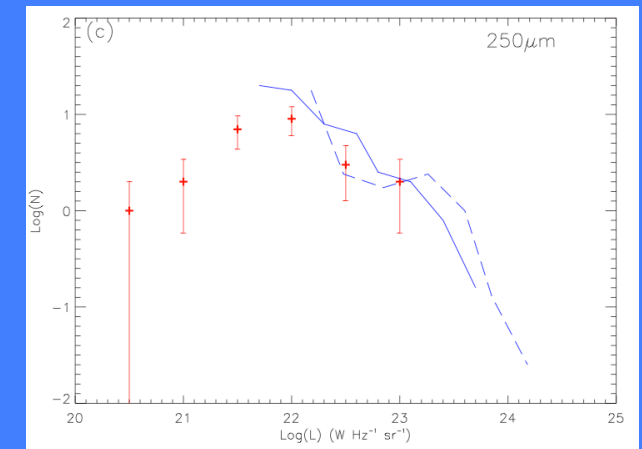
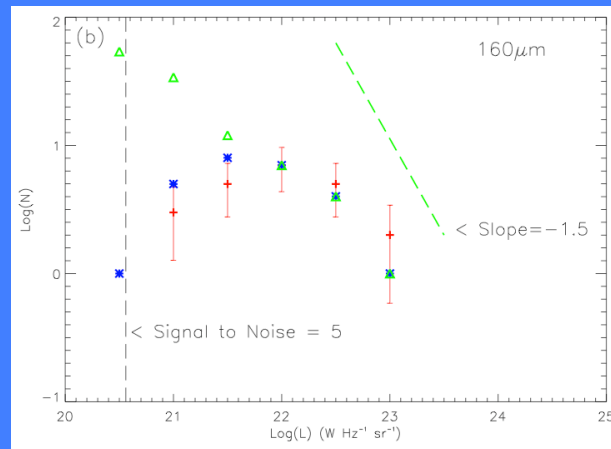
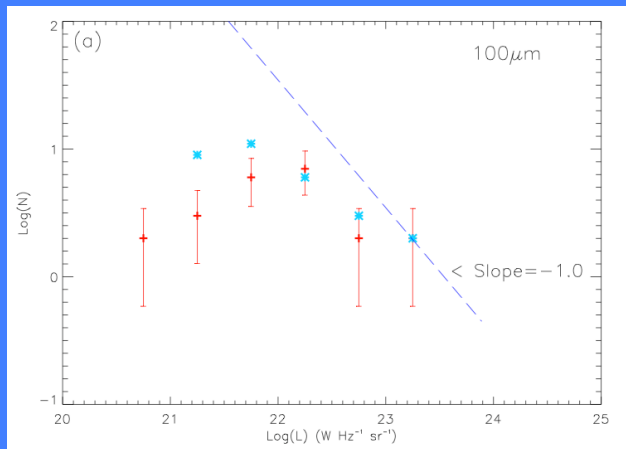
1. Star formation hidden by dust.
2. The energy balance – energy produced by dust.
3. Spectral energy distributions – how much reprocessed by dust.
4. Processes in the inter-stellar medium – dust production.
5. Dust in elliptical galaxies.
6. The mass of cold dust.
7. Environmental effects on dust content of galaxies in clusters.
8. The detection of dust in dwarf galaxies.
9. Dust in the inter-galactic medium.
10. Background galaxies.
11. Unusual objects.



SD papers

The Herschel Virgo Cluster Survey. I. Luminosity functions

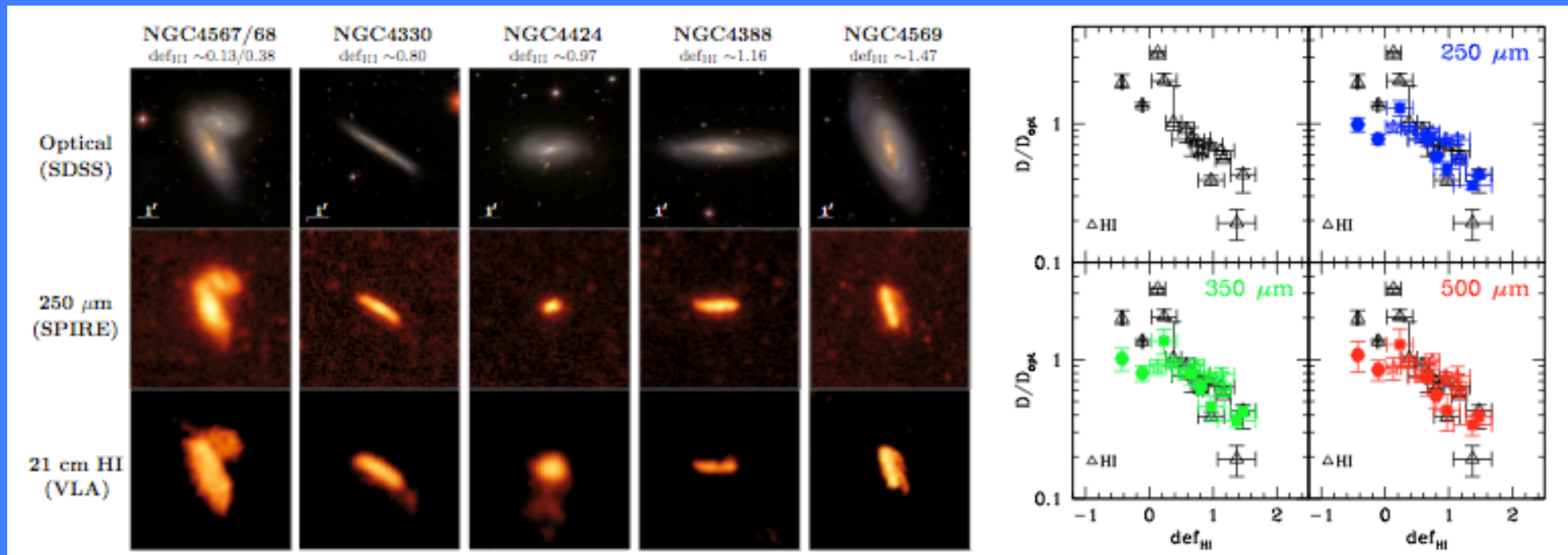
SPIRE and PACS photometry data to produce 100, 160, 250, 350 and 500 μm luminosity functions for optically bright galaxies that are selected at 500 μm and detected in all bands.



SD papers

The Herschel Virgo Cluster Survey . II. Truncated dust disks in H I-deficient spirals

We show for the first time that the extent of the dust disk is significantly reduced in Hi-deficient galaxies, following remarkably well the observed “truncation” of the Hi disk. The cluster environment is able to strip dust as well as gas.



$$def_{HI} = \langle \log M_{HI}(D,T) \rangle - \log M_{HI}(D,T)_{obs}$$

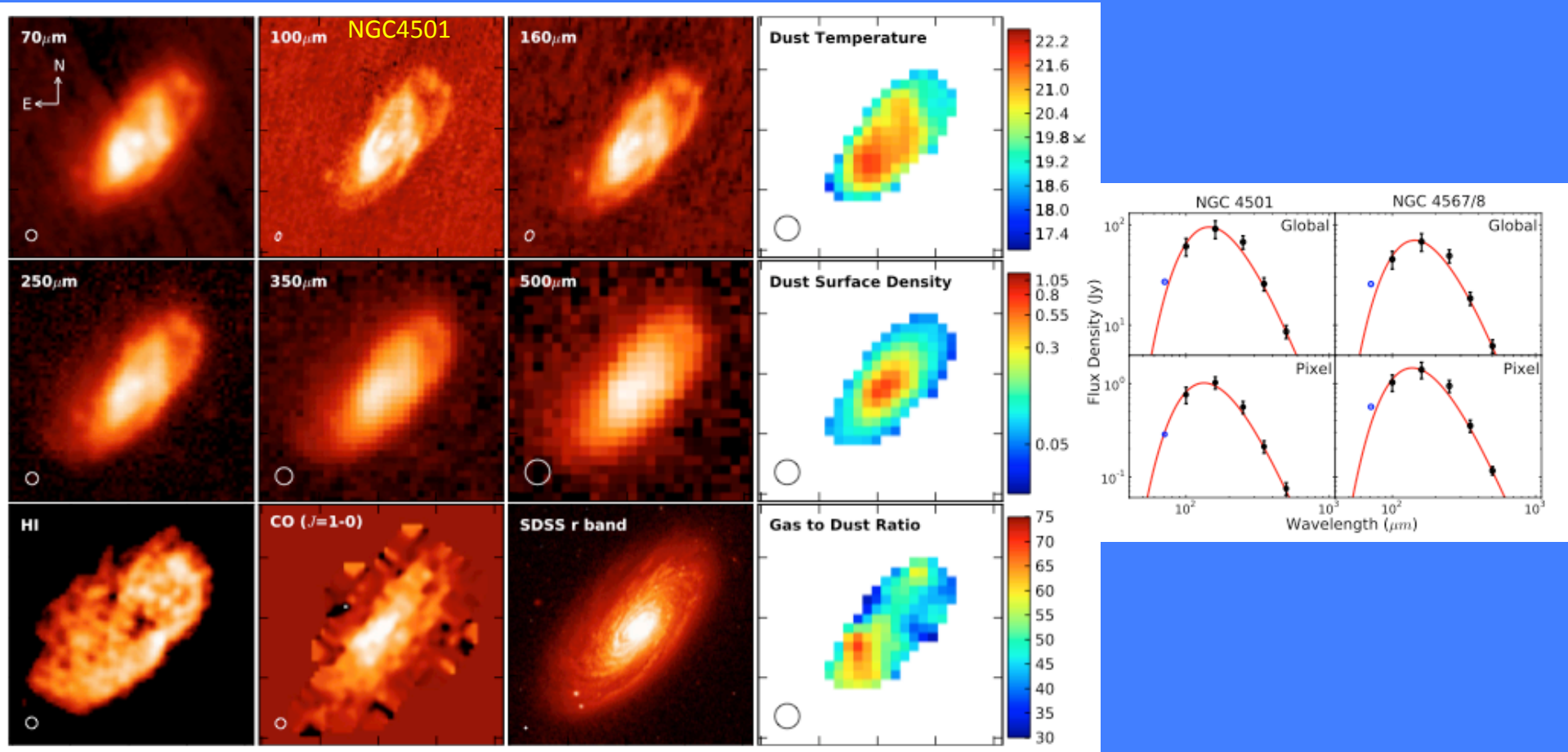
The Herschel Virgo Cluster Survey. III. A constraint on dust grain lifetime in early-type galaxies

Passive early-type galaxies (ETGs) are an ideal laboratory for studying the interplay between dust formation around evolved stars and its subsequent destruction in a hot gas. Using Spitzer-IRS and Herschel data we compare the dust production rate in the envelopes of evolved AGB stars with a constraint on the total dust mass. ETGs which appear to be truly passively evolving are not detected by Herschel. We thus derive a distance independent upper limit to the dust grain survival time in the hostile environment of ETGs of $<46 \pm 25$ Myr for amorphous silicate grains. This implies that ETGs which are detected at far-infrared wavelengths have acquired a cool dusty medium via a relatively recent interaction.

SD papers

The Herschel Virgo Cluster Survey. IV. Resolved dust analysis of spiral galaxies

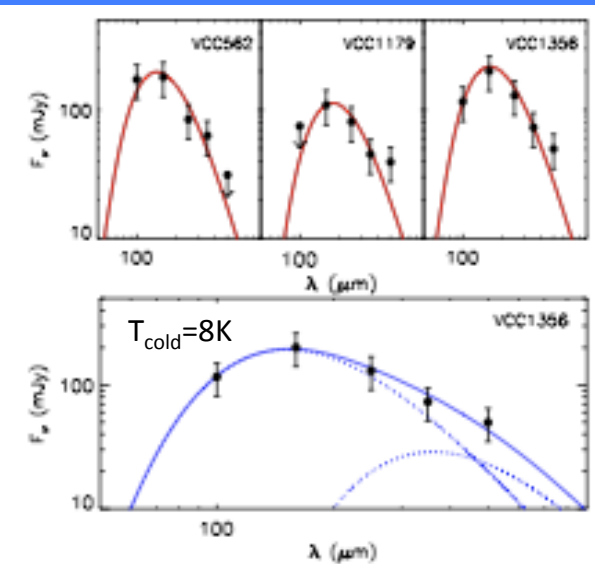
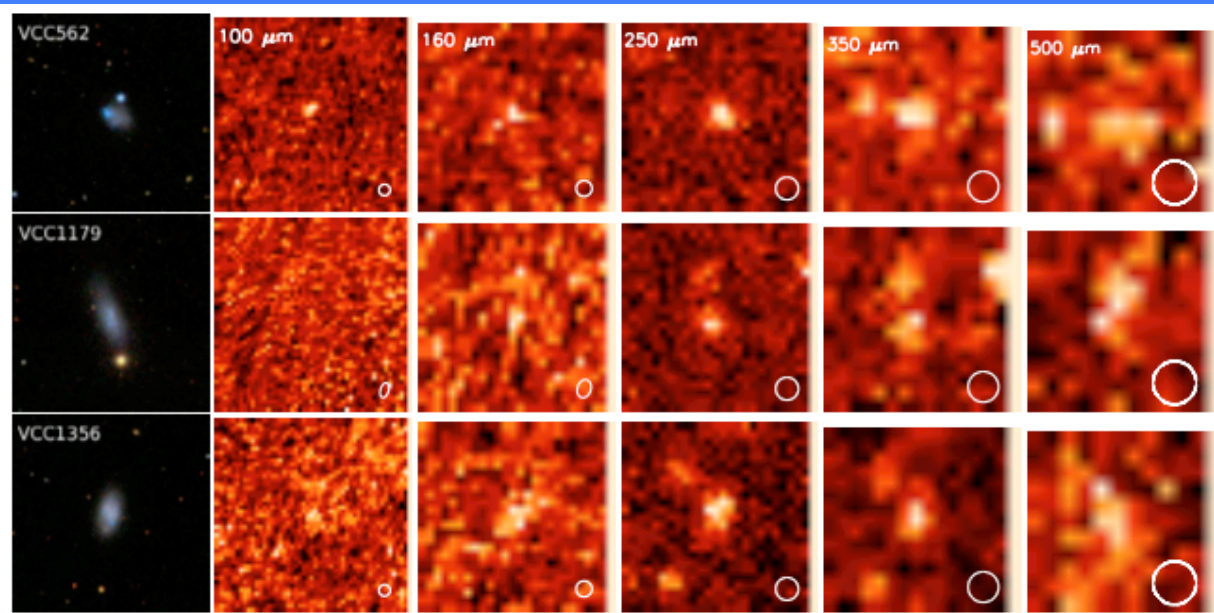
Herschel has unprecedented spatial resolution at far-infrared wavelengths and with the PACS and SPIRE instruments samples both sides of the peak in the far infrared spectral energy distribution (SED). We present maps of dust temperature, dust mass, and gas-to-dust ratio, produced by fitting modified black bodies to the SED for each pixel.



SD papers

The Herschel Virgo Cluster Survey. V. Star-forming dwarf galaxies - dust in metal-poor environments

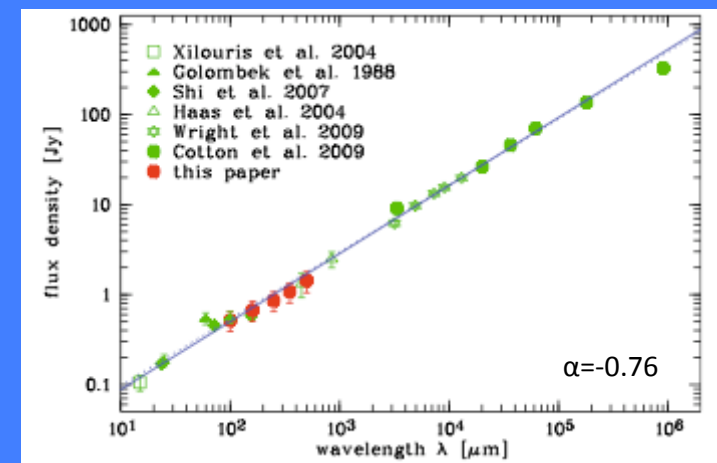
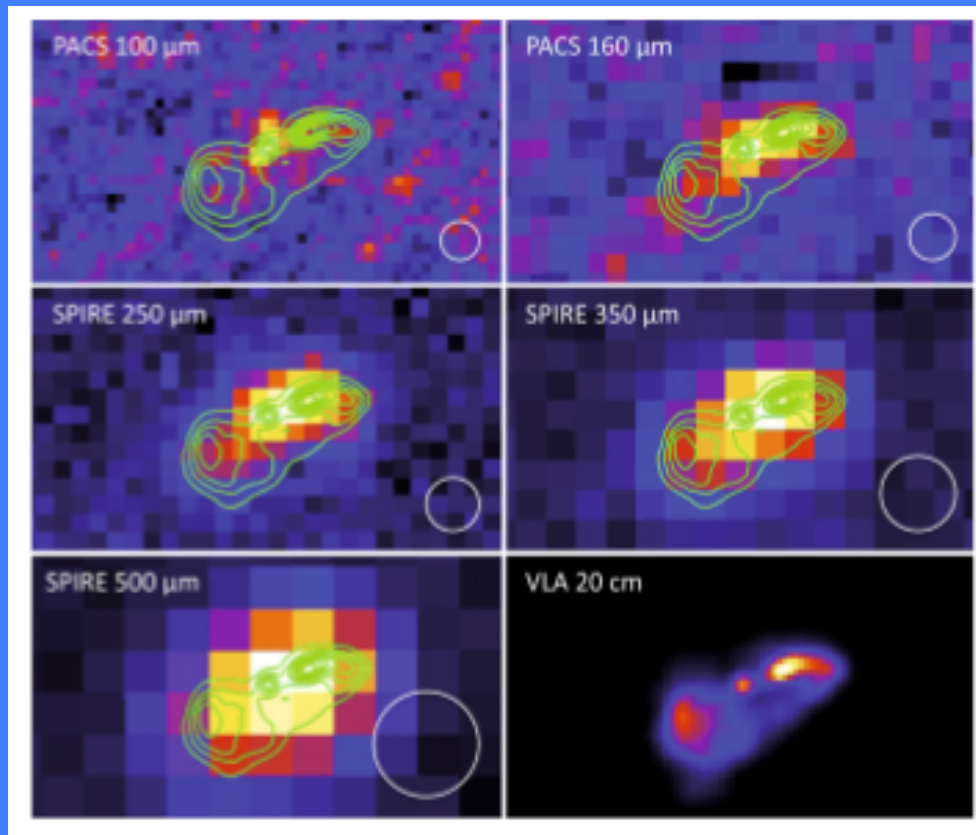
The dust properties of three Virgo cluster star forming dwarf galaxies. These galaxies have low metallicities ($7.8 < 12 + \log(\text{O}/\text{H}) < 8.3$) and star-formation rates $\lesssim 10^{-1} M_{\odot} \text{ yr}^{-1}$. We measure the spectral energy distribution (SED) from 100 to 500 μm and derive dust temperatures and dust masses. The SEDs are fitted by a cool component of temperature $T \lesssim 20 \text{ K}$, implying dust masses around $10^5 M_{\odot}$ and dust-to-gas ratios within the range 10^{-3} - 10^{-2} .



SD papers

The Herschel Virgo Cluster Survey . VI. The far-infrared view of M 87

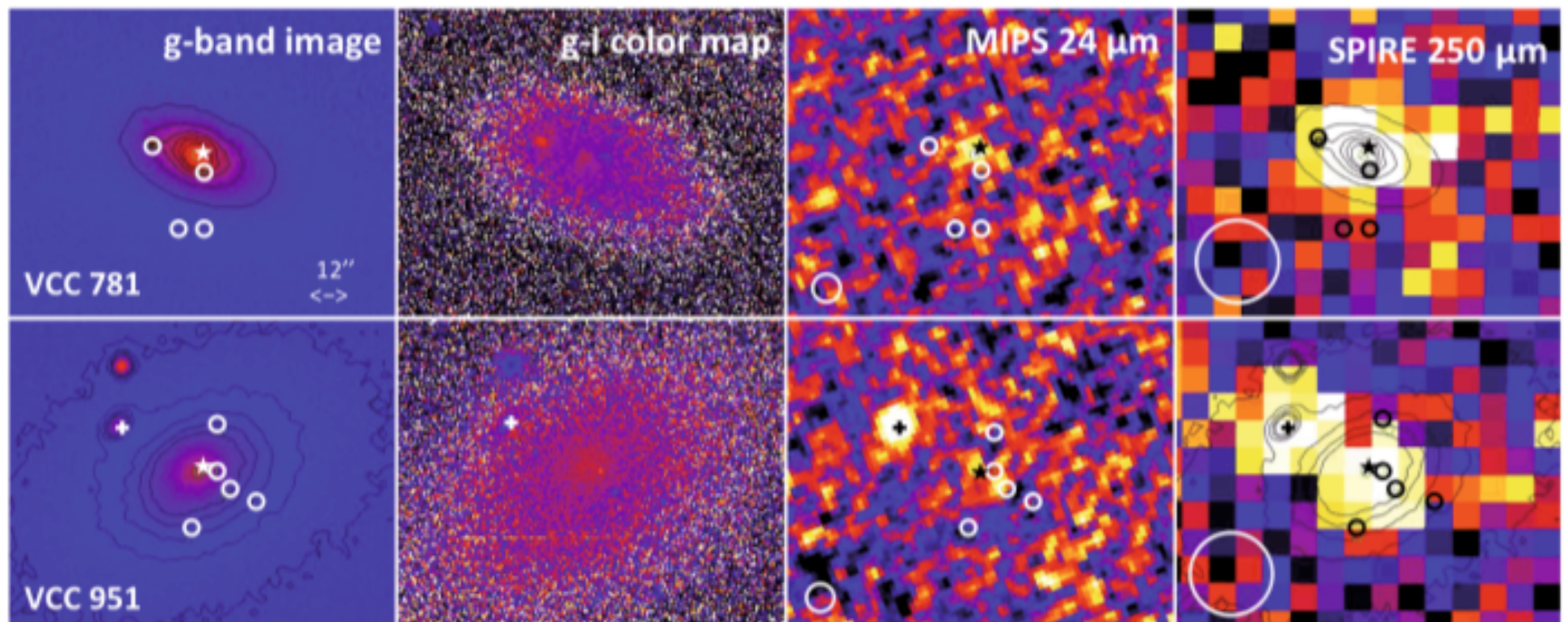
We compare Herschel data with a synchrotron model based on mid-infrared, far-infrared, sub-mm and radio data to investigate the origin of the far-infrared emission. Both the integrated SED and the Herschel surface brightness maps are adequately explained by synchrotron emission. At odds with previous claims, we find no evidence of a diffuse dust component in M 87.



SD papers

The Herschel Virgo Cluster Survey . VII. Dust in cluster dwarf elliptical galaxies

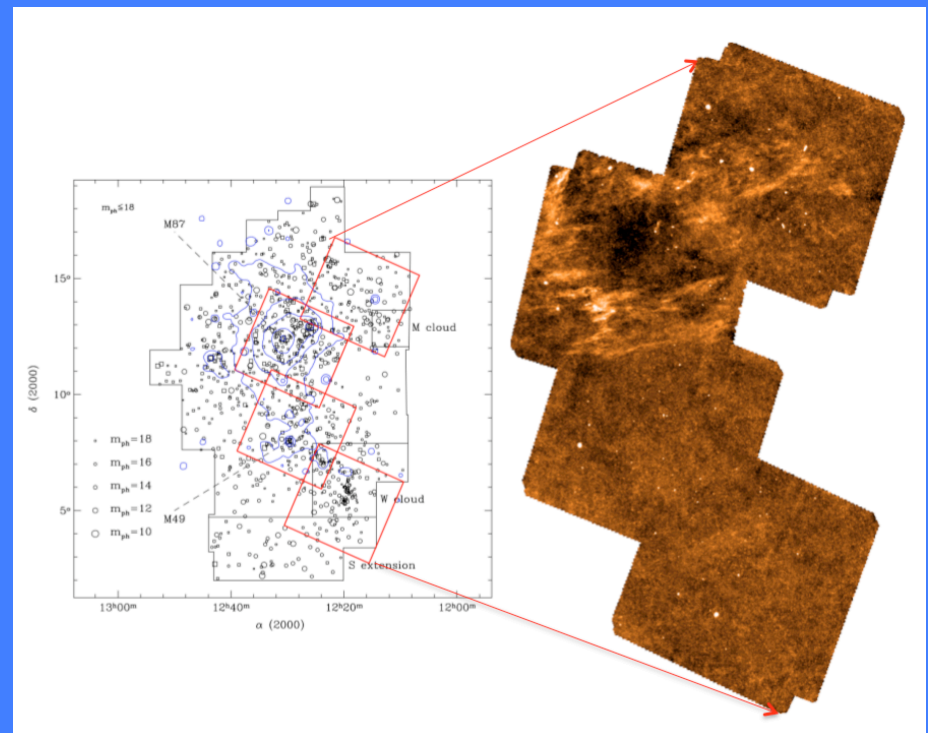
We present the first far-infrared detection of cluster early-type dwarf galaxies: VCC 781 and VCC 951 are detected at the 10σ level in the SPIRE 250 μm image. Both galaxies have dust masses of the order of $10^5 M_{\odot}$ and average dust temperatures ≈ 20 K. The detection rate ($\approx 1\%$) is similar to that for HI emission ($\approx 2\%$). We conclude that the removal of interstellar dust from dwarf galaxies resulting from ram pressure stripping, harassment, or tidal effects must be as efficient as the removal of interstellar gas.



Data release 3 papers

The Herschel Virgo Cluster Survey. VIII. The Bright Galaxy Sample

1. Two scan data that cover all four fields.
2. Sample of 78 bright Virgo galaxies selected at 500μ
3. Calibration checks.
4. Cluster galaxy luminosity distributions.
5. Comparison of the cluster luminosity density in stars and dust (3:1).
6. Mean optical depth for a photon (0.4).
7. Dust masses and temperatures.
8. Stars:gas(atomic) and gas(atomic):dust (mean 15 and 58).
9. Dust[37], gas(atomic)[6] and stellar[32] densities compared to the field.
10. A simple chemical evolution model.
11. Tables of fluxes, masses etc.



Calibration checks with IRAS, ISO, Spitzer and Planck

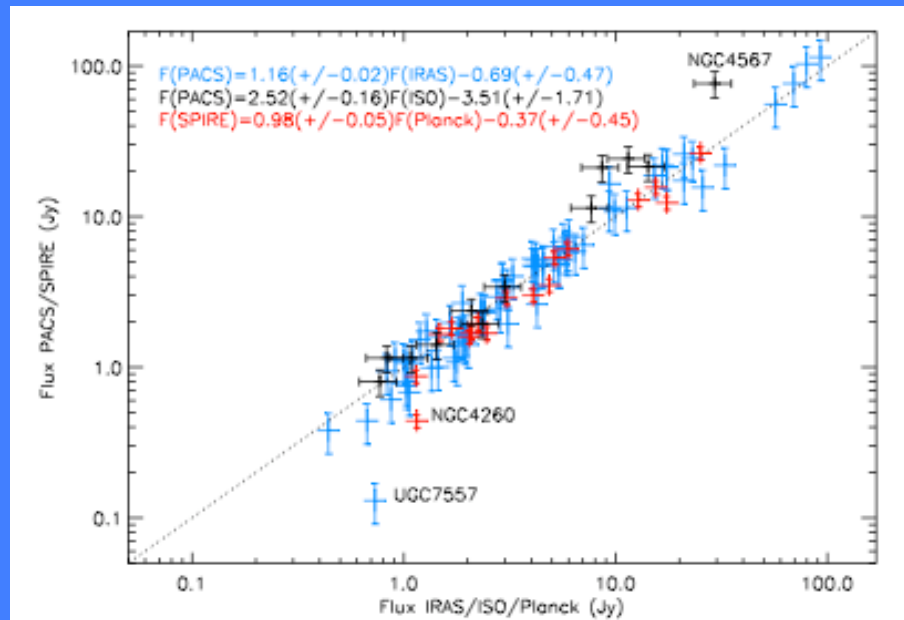


Figure 2. A comparison of IRAS (blue) and ISO (black) fluxes with the PACS 100 μm fluxes along with the Planck/SPIRE 350 μm fluxes. Linear least squares fit parameters are given top left. The black dashed line is the one to one relationship.

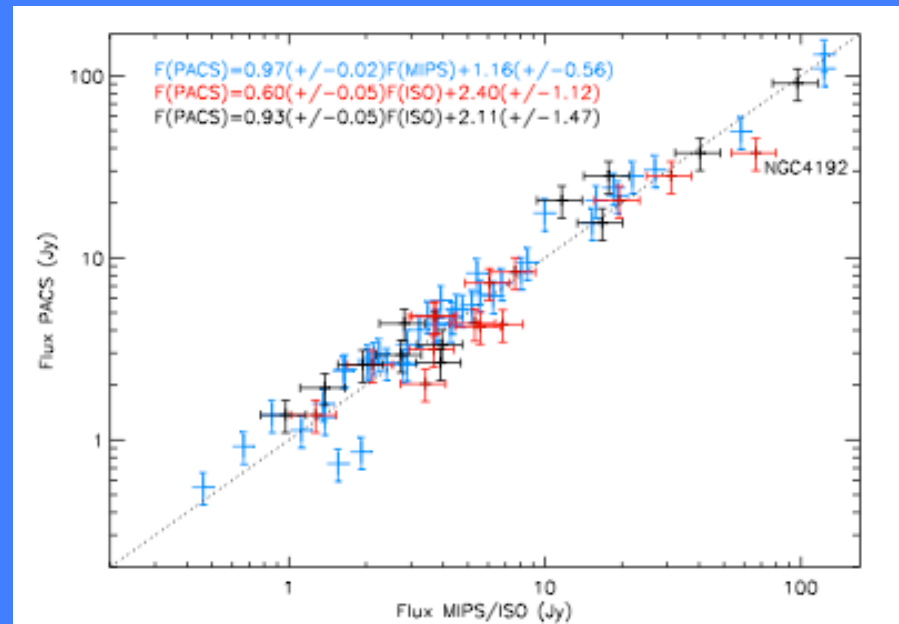


Figure 3. A comparison of the Spitzer (MIPS) 160 μm (blue), the Stickel et al. ISO 170 μm (red) and the Tuffs et al. ISO 170 μm (black) fluxes with the PACS 160 μm fluxes. Linear least squares fit parameters are given top left. The black dashed line is the one to one relationship.

The distribution of luminosities in each band

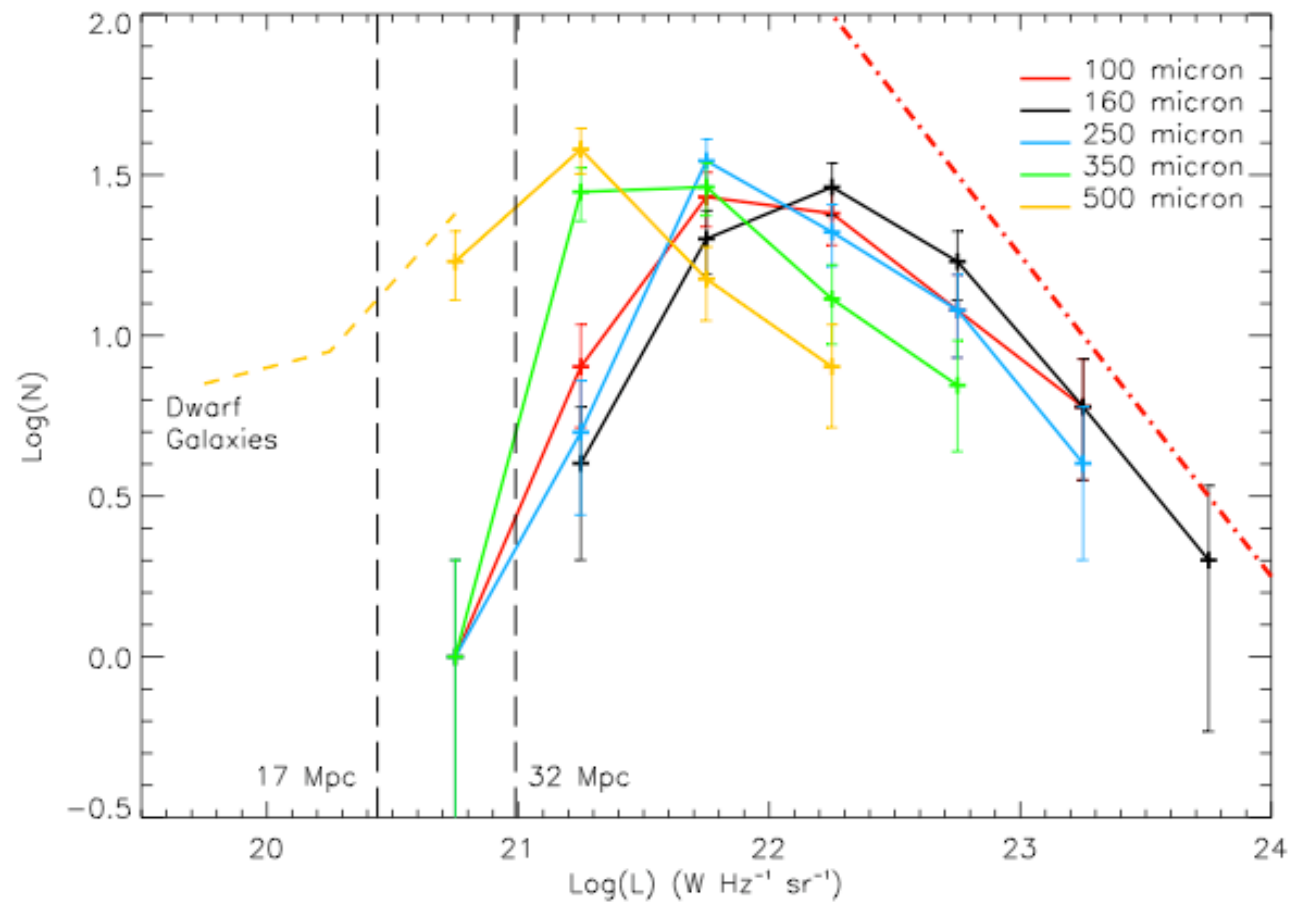
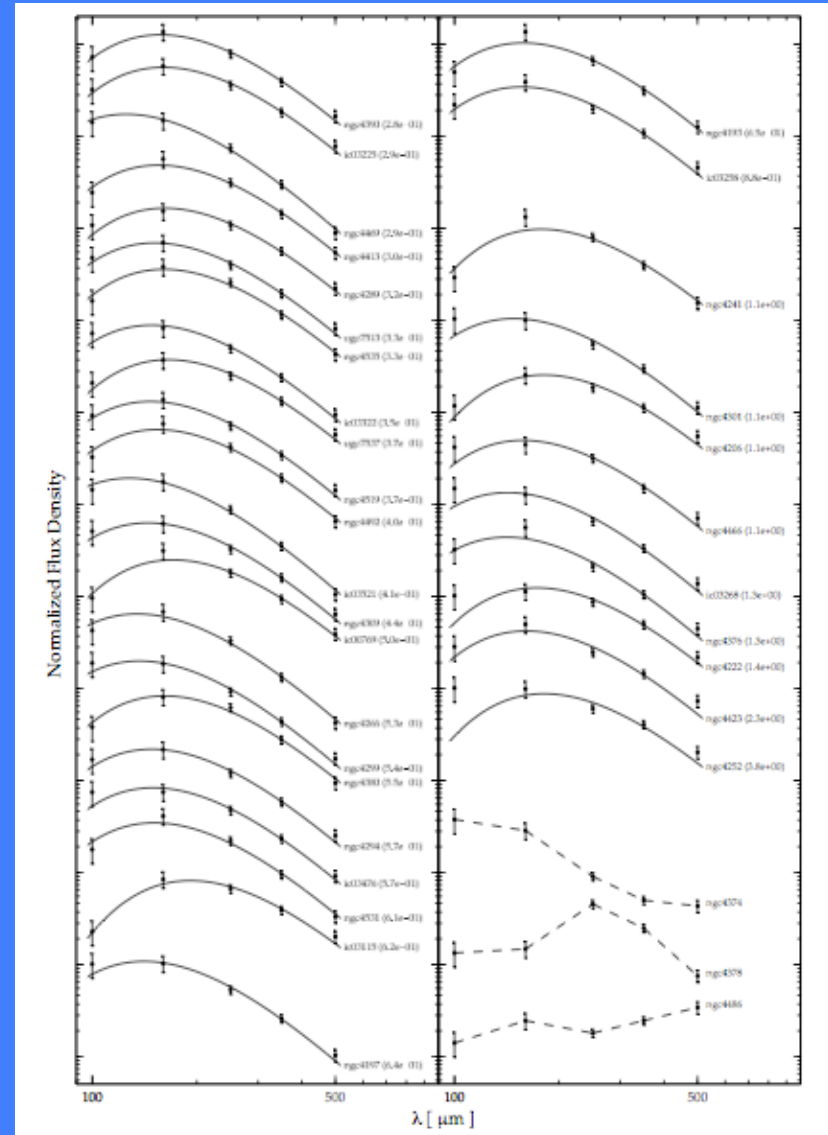
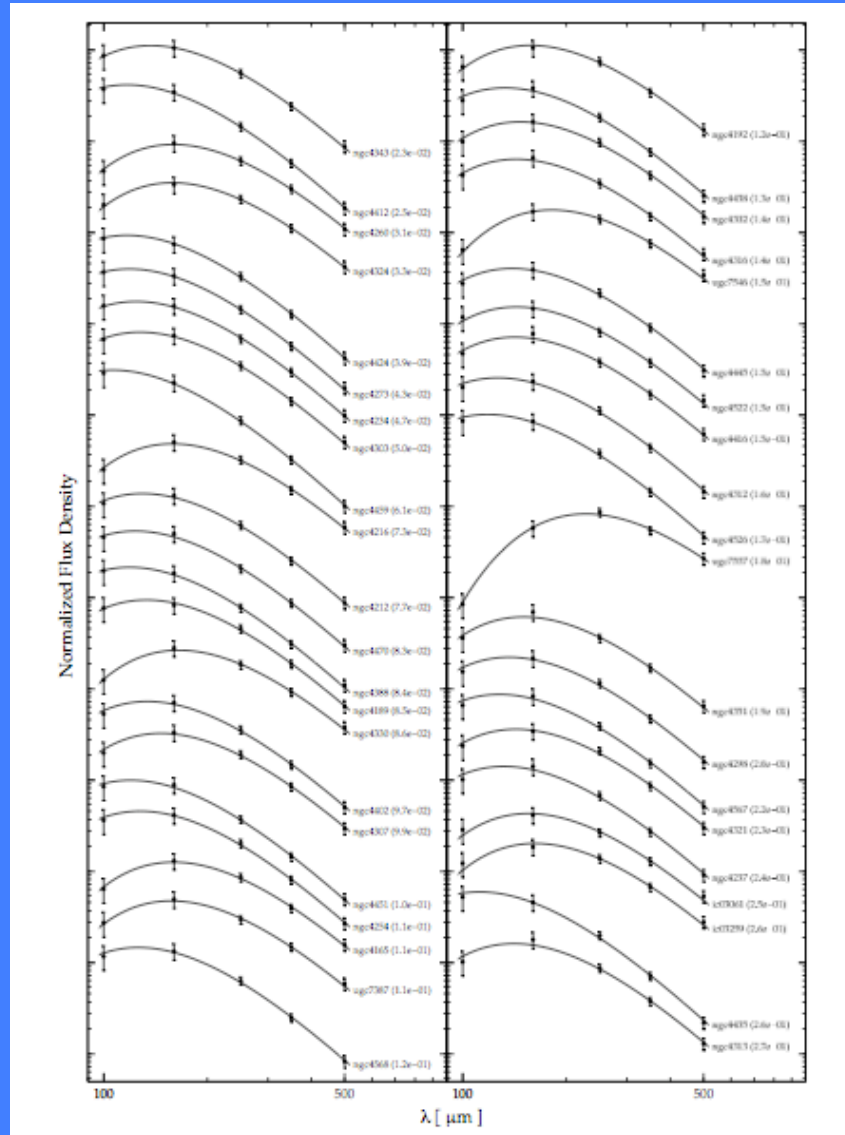
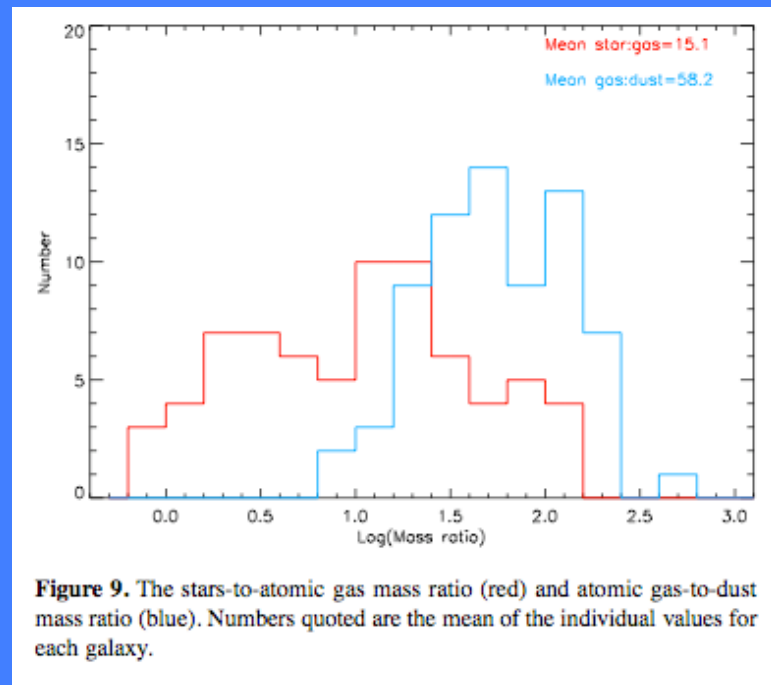
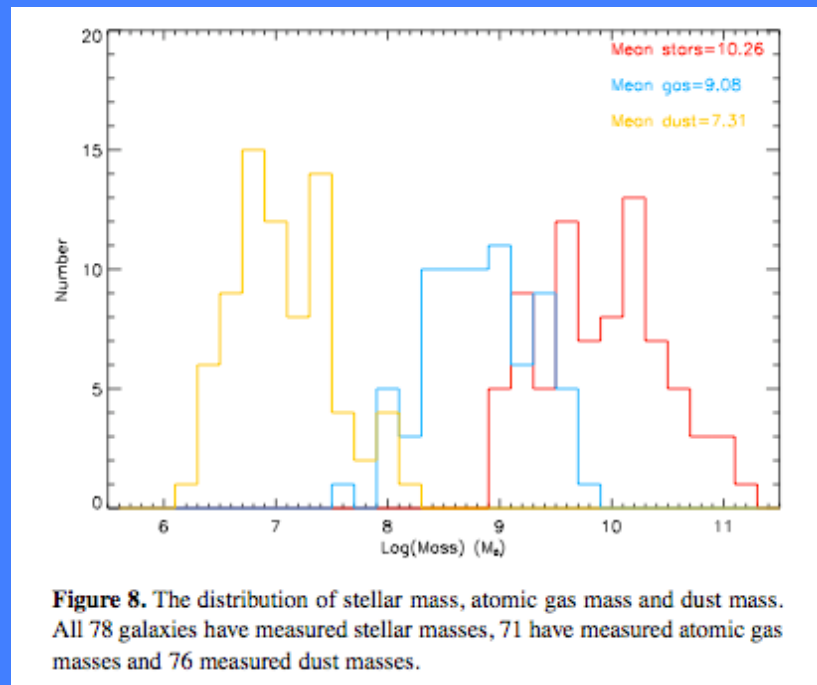
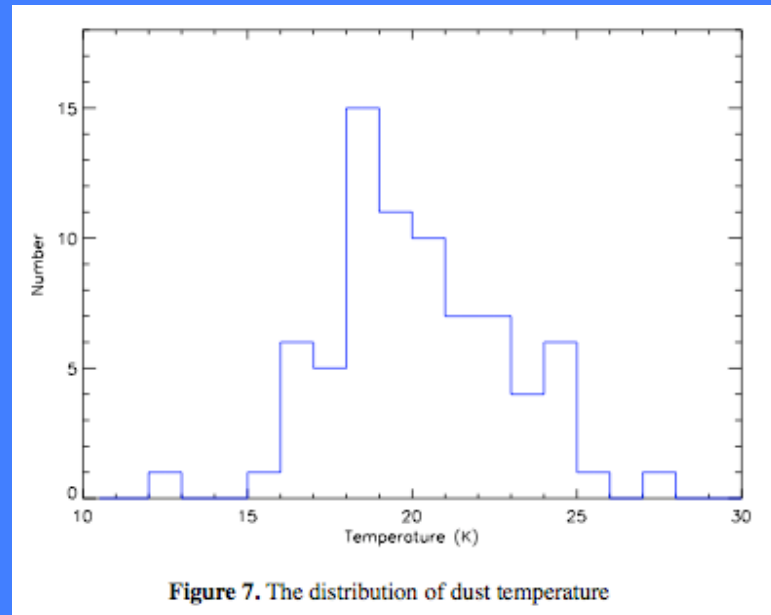


Figure 4. The luminosity distributions derived from the data listed in table 1. The dot-dashed line indicates a slope of -1 as found by Rowan-Robinson et al. (1987) using IRAS 100 μm data. The vertical black dashed lines indicate the minimum luminosity at 17 and 32 Mpc for a minimum 500 μm flux density of 0.1 Jy. The yellow dashed line indicates the shape of the 500 μm luminosity distribution if known star forming dwarf galaxies, beyond our detection limit, are included.

Spectral energy distributions



Various distributions of properties



Various tables of data

(1) Name	(2) RA (J2000)	(3) Dec (J2000)	(4) v (km s ⁻¹)	(5) D (Mpc)	F_{500} (Jy)	F_{350} (Jy)	(6) F_{250} (Jy)	F_{160} (Jy)	F_{100} (Jy)
NGC4165	12:12:12.6	13:14:40.0	1862	32.0	0.15	0.38	0.81	1.19	0.61
IC00769	12:12:32.6	12:07:22.1	2209	32.0	0.40	0.96	1.81	3.04	0.99
NGC4189	12:13:47.8	13:25:32.1	2114	32.0	0.99	2.88	6.91	12.26	11.34
NGC4192	12:13:48.4	14:54:00.5	-139	17.0	5.07	12.87	27.75	37.65	24.24
NGC4193	12:13:53.7	13:10:22.0	2470	32.0	0.68	1.68	3.51	6.93	2.62
NGC4197	12:14:38.8	05:48:23.0	2062	32.0	0.67	1.68	3.37	6.37	6.32
IC03061	12:15:04.6	14:01:42.9	2316	17.0	0.32	0.77	1.56	2.35	1.68
NGC4206	12:15:17.1	13:01:28.4	704	17.0	1.08	2.20	3.56	4.69	2.35
NGC4212	12:15:39.0	13:54:08.7	-88	17.0	1.85	5.33	12.96	26.77	21.78

(1) Name	(2) M_B	(3) $\text{Log}(M_{\text{Stars}})$ (M_{\odot})	(4) $\text{Log}(M_{\text{HI}})$ (M_{\odot})	(5) $\text{Log}(M_{\text{Dust}})$ (M_{\odot})	(6) T_d (K)	(7) $\text{Log}(L_{0.4-2.5})$ (L_{\odot})	(8) $\text{Log}(L_{100-500})$ (L_{\odot})	(9) $\langle \tau \rangle$	(10) $M_{\text{Stars}}/M_{\text{HI}}$	(11) $M_{\text{HI}}/M_{\text{Dust}}$
NGC4165	-17.99	9.77	8.39	6.97±0.07	18.2±0.9	9.67	8.93	0.17	24.0	26.3
IC00769	-19.13	9.98	9.48	7.44±0.07	17.0±0.8	9.71	9.26	0.30	3.2	109.6
NGC4189	-19.84	10.39	9.40	7.65±0.07	21.8±1.3	10.08	10.05	0.66	9.8	56.2
NGC4192	-20.42	10.88	9.63	7.93±0.07	18.4±0.9	10.56	9.93	0.21	17.8	50.1
NGC4193	-19.24	10.29	9.24	7.60±0.07	18.4±0.9	10.11	9.62	0.28	11.2	43.7
NGC4197	-19.15	9.91	9.71	7.46±0.08	20.6±1.3	9.80	9.79	0.68	1.6	177.8
IC03061	-16.77	9.23	8.79	6.69±0.08	18.7±1.0	9.08	8.74	0.37	2.8	125.9
NGC4206	-18.15	9.72	9.38	7.31±0.08	16.1±0.8	9.63	8.99	0.21	2.2	117.5

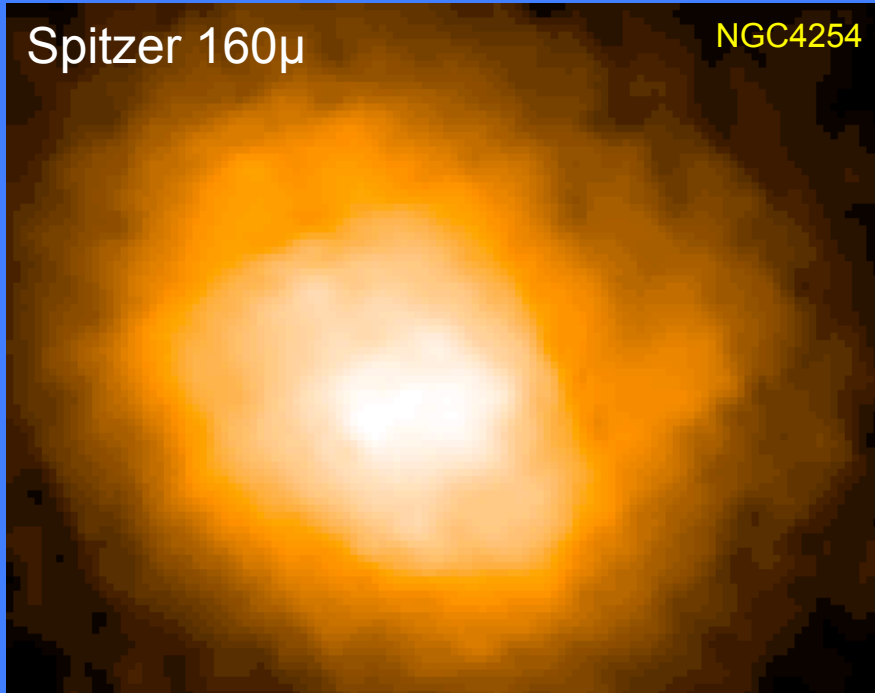
Other papers submitted

The Herschel Virgo Cluster Survey. IX. Dust-to-gas mass ratio and metallicity gradients in four Virgo spiral galaxies

The Herschel Virgo Cluster Survey: X. The relationship between cold dust and molecular gas content in Virgo spirals[★]

Spitzer 160 μ

NGC4254



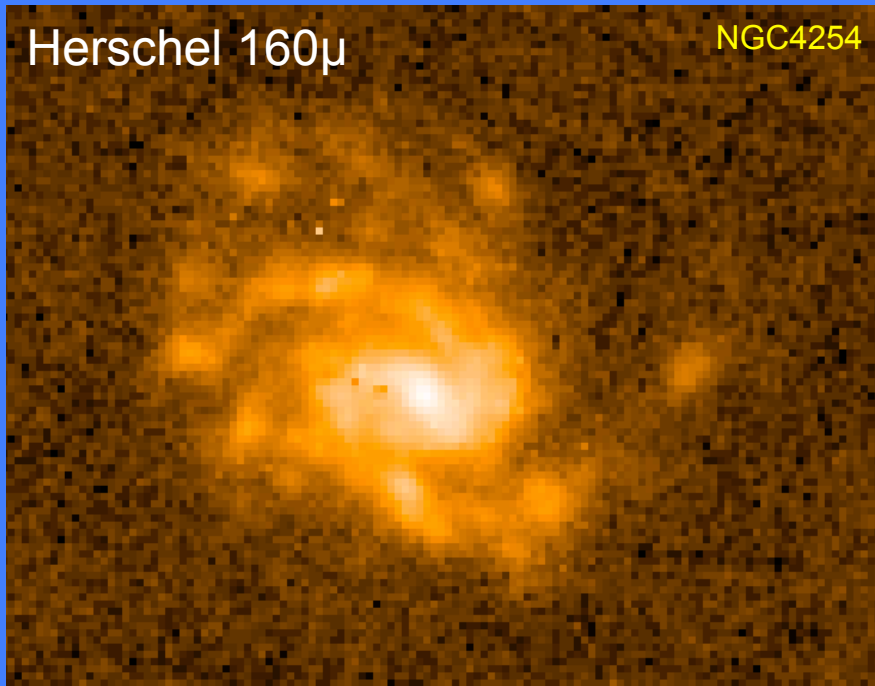
Current status

Data release 3 to the consortium consists of two orthogonal scans of all four fields.

Hopefully all eight scans completed very soon (July?).

Herschel 160 μ

NGC4254



Final data products after data reduction and quality checks lasting 2-3 months.